Coherent generation of time-bin entangled photon pairs using the biexciton cascade and cavity-assisted piecewise adiabatic passage

P. K. Pathak[1,2] and S. Hughes[2]

[1]*School of Basic Sciences, Indian Institute of Technology, Mandi 175 001, India*

[2]*Department of Physics, Queen's University, Kingston, Ontario, Canada K7L 3N6*

(Received 8 October 2010; revised manuscript received 8 March 2011; published 3 June 2011)

We present a scheme to realize a deterministic solid-state source of time-bin entangled photon pairs using cavity-assisted piecewise adiabatic passage in a single quantum dot. The quantum dot is embedded inside a semiconductor microcavity, and the interaction of a coherent superposition of two temporally separated input pulses and the cavity mode leads to a piecewise adiabatic passage, which produces a time-bin entangled photon pair through the biexciton-exciton cascade. We show that the entanglement of the generated state can be measured using triple coincidence detection, and we quantify the degree of entanglement through the visibility of the interference. We also discuss the influence of pure dephasing on the entanglement of the generated photon pair. Pronounced interference visibility values of greater than $1/\sqrt{2}$ are predicted in triple coincidence measurement using experimentally achievable parameters, demonstrating that the generated photons could be suitable for applications such as Bell's inequality violation and quantum cryptography.

DOI: 10.1103/PhysRevB.83.245301 PACS number(s): 03.65.Ud, 03.67.Mn, 42.50.Dv

I. INTRODUCTION

A source of entangled photon pairs is an essential building block for various quantum-information processing protocols,[1] such as quantum cryptography[2] and quantum teleportation.[3] Generally, the employed entangled state of photons in these experiments are entangled in the energy and the polarization degrees of freedom.[4] However, because of unavoidable polarization dispersion in optical fibers, the polarization entangled photons are not suitable for distribution over large distances. In related experiments,[5–8] entangled states of photons in energy and time degrees of freedom, using discrete time interval (time bin) for photon emission, have been demonstrated and the entanglement between these photons has been successfully distributed over a distance of 50 km.[8] In these experiments, the time-bin entangled photons were generated through a parametric down convertor (PDC) using the pump as a superposition of two time separated pulses. A PDC is a heralded source of entangled photons where the number of generated photon pairs are probabilistic.[9] At low pump intensity, when the probability of generating more than one photon pair remains small, the efficiency of the source remains very low (less than 20%[7]). For quantum-information processing applications,[10] one requires a scalable source that generates precisely a single photon pair "on demand." In the past few years, there has been considerable progress for developing indistinguishable single photon sources[11] and entangled photon sources[12–14] using single quantum dots (QDs), where the QDs provide the potential advantages of integrability and scalability in such experiments. In semiconductor QDs, polarization entangled photons have been successfully generated in the biexciton-exciton cascade decay.[12–14]

In 2005, Simon and Poizat[15] proposed the generation of a single time-bin entangled photon pair through the biexciton-exciton cascade decay in idealized QDs, where the biexciton state is created by pumping through two pulses interacting at two distinct times. The state of the time-bin entangled photon pair is subsequently given by $|\psi\rangle = \sqrt{p_1}|\text{early}\rangle_1|\text{early}\rangle_2 + e^{i\theta}\sqrt{p_2}|\text{late}\rangle_1|\text{late}\rangle_2$, where early and late are two time bins, p_1 is the probability of generating a photon pair in the early time bin (from the first pulse), and p_2 is the probability of generating a photon pair in the late time bin (from the second pulse); the total probability of generating the photon pair is then $p_1 + p_2 = 1$. For generating a maximally entangled state $|\psi\rangle$, one requires $p_1 = p_2 = 1/2$. Therefore, a precisely regulated population transfer between the QD energy levels is essential. The above picture is highly idealized, and to our knowledge there have been no experimental demonstrations of generating time-bin entangled pairs in QDs. To assess the feasibility of time-bin entanglement in real QDs, one requires realistic models with experimentally accessible parameters. For example, pure dephasing processes present in semiconductor systems are known to produce detrimental effects on the entanglement of the generated state. In quantum-information protocols, such as entanglement swapping, it is also essential that the photons should not have any other correlation except the time-bin entanglement. However, in the biexciton-exciton cascade, emitted photons also have time correlations. These undesirable temporal correlations can be minimized by carefully manipulating the emission rates of the emitted photons.[15]

In this work, we introduce a coherent excitation scheme to efficiently generate a time-bin entangled photon pair using cavity-assisted piecewise adiabatic passage (CAPAP). Cavity-assisted stimulated Raman adiabatic passage (STIRAP) has been successfully implemented for generating single photon sources,[16] where the cavity mode acts as a constant Stokes field. In the conventional STIRAP, population from the initial state to the final state is completely transferred by a pair of slowly varying pump and Stokes pulses. The system evolves adiabatically along one of its time-dependent dressed states, which coincides with the initial state at the initial time and with the final state after the time evolution. In a piecewise adiabatic passage, the pump and the Stokes pulses are replaced by a series of pulses and each pair of the pump and Stokes pulses transfers a fraction of population from the initial state

to the final state. The *piecewise adiabatic passage* has been found equally robust as the conventional STIRAP and does not depend on the time interval between the pulses and their shapes as long as the adiabatic condition is fulfilled.[17] The piecewise adiabatic passage for the complete population transfer using a series of pulses has been recently demonstrated in atomic experiments.[17] In our proposal, we replace the Stokes pulse by a cavity field and the pump pulse by a superposition of two pulses, which is an extension of the cavity-assisted adiabatic passage to the CAPAP. Also, the cavity field couples the ground state to the biexciton state through two photon transition via intermediate exciton state $|y\rangle$. In terms of related experiments, the coherent excitation in semiconductor QD cavities has been an active area of recent research.[18–22]

In our proposal, we consider the initial state of the QD as a metastable or relatively long-lived state, and there could be two possibilities for achieving this: either using a dark exciton state[23] or using an off-resonant exciton in a photonic band-gap crystal which results in a long radiative decay.[24] Through cavity coupling and strategic coherent pulse excitation, we demonstrate that the CAPAP process in a QD can provide an efficient way for population transfer, which in turn can be used to generate time-bin entangled photon pairs *on demand*. We also investigate how the cavity-enhanced decay rates suppress the detrimental effects of pure dephasing.

Our paper is organized as follows. In Sec. II, we present a formal theory of the generation of a time-bin entangled photon pair from a single QD coupled to a semiconductor cavity. In Sec. III, we investigate the measure of photon entanglement by a triple coincidence detection and also study the influence of QD pure dephasing. In Sec. IV, we conclude.

II. GENERATING TIME-BIN ENTANGLED PHOTON PAIRS USING CAPAP

We consider a QD embedded in a semiconductor microcavity, where the energy-level diagram of the system is shown in Fig. 1. The dipole transitions from the biexciton state $|u\rangle$ to the exciton state $|y\rangle$, and from the exciton state $|y\rangle$ to the ground state $|g\rangle$, are coupled through a y-polarized single mode of the semiconductor cavity, with coupling constants g_1 and g_2, respectively. Because of the large biexciton binding energy of semiconductor QDs, it is generally not possible to couple the biexciton and exciton transitions from the same cavity mode, and thus manipulation of the biexciton binding energy becomes essential in these systems.[25,26] Usually the binding energy of the charge-neutral biexciton has a negative value; however, by changing the QD confinement size[27] or by changing the strain,[28] it has been found that the biexciton binding energy can be tuned to zero or a positive value. Very recently, manipulation of the binding energy of the biexciton has also been reported by applying lateral electric fields.[26,29] Moreover, construction of an electrode for applying a lateral electric field in the vicinity of a QD within a photonic crystal cavity has also been reported.[30]

For simplicity, we assume that the QD is initially prepared in the metastable state $|m\rangle$ and the cavity mode is in the vacuum state. We consider two possibilities for the metastable or long-lived state: (i) a dark exciton[23] or (ii) an off-resonant exciton embedded in a (planar) photonic band-gap structure.

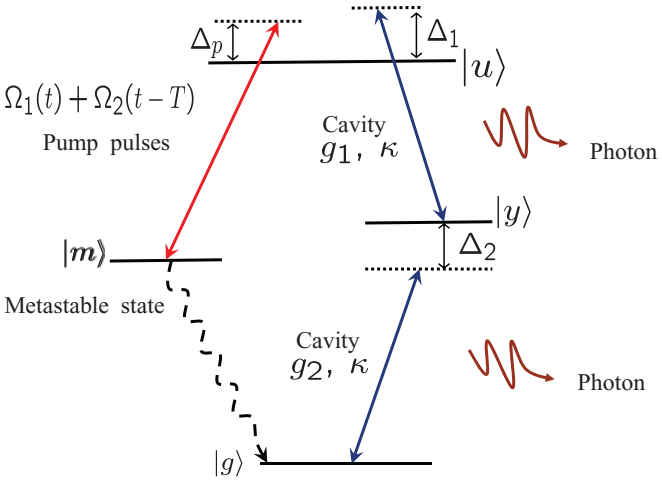

FIG. 1. (Color online) Schematic diagram for time-bin entangled photon generation. The transitions from the biexciton state $|u\rangle$ to the exciton states $|y\rangle$ and $|y\rangle$ to ground state $|g\rangle$ are coupled by a y-polarized cavity mode. The QD is pumped from the metastable (or long lived) state $|m\rangle$ to the biexciton state through the superposition of two input pulses.

The later long-lived exciton decay has been observed in recent experiments; e.g., Hennessy *et al.*[24] have measured the decay rate for the off-resonant exciton in the photonic crystal much less than 10^{-3} times of the cavity-mode coupling strength ($\sim$0.05 μeV), and our calculations will show that such relatively long lifetimes can be exploited to efficiently generate time-bin entangled photon pairs. An x-polarized pump field with a Rabi frequency $\Omega_p(t)$ is applied between the metastable state $|m\rangle$ and the biexciton state $|u\rangle$. The Hamiltonian of the system in the rotating frame can be written as

$$H = \hbar\Delta_p|m\rangle\langle m| + \hbar\Delta_1|y\rangle\langle y| + \hbar(\Delta_1+\Delta_2)|g\rangle\langle g| + \hbar[\Omega_p(t)|u\rangle\langle m| + g_1|u\rangle\langle y|a + g_2|y\rangle\langle g|a + \text{H.c.}], \quad (1)$$

where Δ_p and Δ_1 (Δ_2) are the detunings of the pump field and the cavity mode with the biexciton (exciton) transition frequencies, respectively; H.c. refers to Hermitian conjugate. For simulating the dynamics of the system, we perform quantum master equation calculations in the density-matrix representation. The evolution of the QD-cavity system is governed by

$$\dot{\rho} = -\frac{i}{\hbar}[H,\rho] - \frac{1}{2}\sum_{\mu}[L_\mu^\dagger L_\mu\rho - 2L_\mu\rho L_\mu^\dagger + \rho L_\mu^\dagger L_\mu], \quad (2)$$

where L_μ are the Lindblad operators, with terms $\sqrt{\gamma_m}|g\rangle\langle m|$, $\sqrt{\gamma_1}|m\rangle\langle u|$, $\sqrt{\gamma_1}|y\rangle\langle u|$, and $\sqrt{\gamma_2}|g\rangle\langle y|$ corresponding to the spontaneous decays and $\sqrt{2\gamma_d}|u\rangle\langle u|$, $\sqrt{\gamma_d}|m\rangle\langle m|$, and $\sqrt{\gamma_d}|y\rangle\langle y|$ corresponding to pure dephasing of the biexciton and exciton states. The emission of the photons from the cavity mode is given by the Lindblad operator $\sqrt{\kappa}a$, where κ is the decay rate of the leaky cavity. We neglect the spontaneous decay of the metastable state $|m\rangle$ in the case of a dark exciton and include a small decay rate $\gamma_m = 10^{-3}g_2$ in the case of an off-resonant exciton.

We numerically solve the optical Bloch equations, using Eq. (2), for density-matrix elements $\rho_{ij} = \langle i|\rho|j\rangle$. To simplify

the notation, we use the definitions $|Y\rangle = |y,1\rangle$, $|G\rangle = |g,1\rangle$, and $|G'\rangle = |g,2\rangle$, where in the alpha-numeric notation, letters correspond to the energy state of QD and numbers correspond to the number of photons in the cavity mode. The complete dynamics of the system is expressed by the following equations of motion:

$$\dot{\rho}_{mm} = -i\Omega_p^*(t)\rho_{um} + i\Omega_p(t)\rho_{mu} + \gamma_1\rho_{uu} - \gamma_m\rho_{mm}, \quad (3a)$$

$$\dot{\rho}_{uu} = i\Omega_p^*(t)\rho_{um} - i\Omega_p(t)\rho_{mu} + ig_1\rho_{uY} - ig_1\rho_{Yu} - 2\gamma_1\rho_{uu}, \quad (3b)$$

$$\dot{\rho}_{YY} = -ig_1\rho_{uY} + ig_1\rho_{Yu} - ig_2\sqrt{2}\rho_{G'Y} + ig_2\sqrt{2}\rho_{YG'} - (\kappa+\gamma_2)\rho_{YY}, \quad (3c)$$

$$\dot{\rho}_{G'G'} = ig_2\sqrt{2}\rho_{G'Y} - ig_2\sqrt{2}\rho_{YG'} - 2\kappa\rho_{G'G'}, \quad (3d)$$

$$\dot{\rho}_{GG} = ig_2(\rho_{Gy}+\rho_{yG}) + 2\kappa\rho_{G'G'} + \gamma_2\rho_{YY} - \kappa\rho_{GG}, \quad (3e)$$

$$\dot{\rho}_{yy} = -ig_2(\rho_{Gy}-\rho_{yG}) + \kappa\rho_{YY} + \gamma_1\rho_{uu} - \gamma_2\rho_{yy}, \quad (3f)$$

$$\dot{\rho}_{gg} = \kappa\rho_{GG} + \gamma_2\rho_{yy} + \gamma_m\rho_{mm}, \quad (3g)$$

$$\dot{\rho}_{um} = -i\Delta_p\rho_{um} - i\Omega_p\rho_{mm} - ig_1\rho_{Ym} + i\Omega_p\rho_{uu} - \left(\gamma_1 + \frac{3\gamma_d+\gamma_m}{2}\right)\rho_{um}, \quad (3h)$$

$$\dot{\rho}_{uY} = -i\Delta_1\rho_{uY} - i\Omega_p\rho_{mY} - ig_1\rho_{YY} + ig_1\rho_{uu} + ig_2\sqrt{2}\rho_{uG'} - \left(\gamma_1 + \frac{\kappa+\gamma_2+3\gamma_d}{2}\right)\rho_{um}, \quad (3i)$$

$$\dot{\rho}_{YG'} = -i\Delta_2\rho_{YG'} - ig_1\rho_{uG'} - ig_2\sqrt{2}\rho_{G'G'} + ig_2\sqrt{2}\rho_{YY} - \left(\frac{3\kappa+\gamma_2+\gamma_d}{2}\right)\rho_{YG'}, \quad (3j)$$

$$\dot{\rho}_{mY} = -i(\Delta_1-\Delta_p)\rho_{mY} - i\Omega_p^*(t)\rho_{uY} + ig_1\rho_{mu} + ig_2\sqrt{2}\rho_{mG'} - \left(\gamma_d + \frac{\kappa+\gamma_2+\gamma_m}{2}\right)\rho_{mY}, \quad (3k)$$

$$\dot{\rho}_{uG'} = -i(\Delta_1+\Delta_2)\rho_{uG'} - i\Omega_p(t)\rho_{mG'} - ig_1\rho_{YG'} + ig_2\sqrt{2}\rho_{uY} - (\gamma_d+\kappa+\gamma_2)\rho_{uG'}, \quad (3l)$$

$$\dot{\rho}_{mG'} = -i(\Delta_1+\Delta_2-\Delta_p)\rho_{mG'} - i\Omega_p^*(t)\rho_{uG'} + ig_2\sqrt{2}\rho_{mY} - \left(\kappa + \frac{\gamma_d+\gamma_m}{2}\right)\rho_{mG'}, \quad (3m)$$

$$\dot{\rho}_{yG} = -i\Delta_2\rho_{yG} - ig_2\rho_{GG} + ig_2\rho_{yy} - \frac{(\kappa+\gamma_2+\gamma_d)}{2}\rho_{yG}. \quad (3n)$$

When the pump field and the cavity mode approximately satisfy the resonance condition,[31] $\Delta_p \approx \Delta_1 + \Delta_2$, the evolution of the population in the QD energy levels follows the CAPAP. Here, one must also remember that the Stark shifts also play an important role in the resonance condition.[31] However, for constant cavity couplings, the Stark shifts of the energy states remain constant and the above resonance condition can be easily satisfied by simply changing the detuning of the pump field (Δ_p) only.

In Fig. 2, we show the numerical simulations after solving Eqs. (3a)–(3n). The pump field is chosen to be a coherent superposition of two time-separated Gaussian pulses of the same width, but different amplitudes, which can be generated by passing a Gaussian pulse through an unbalanced two-arm interferometer. The Rabi frequency of the pump field is given by $\Omega_p(t) = \Omega_1(t) + \Omega_2(t-T)$, where $\Omega_{1,2}(t)$ is the Rabi

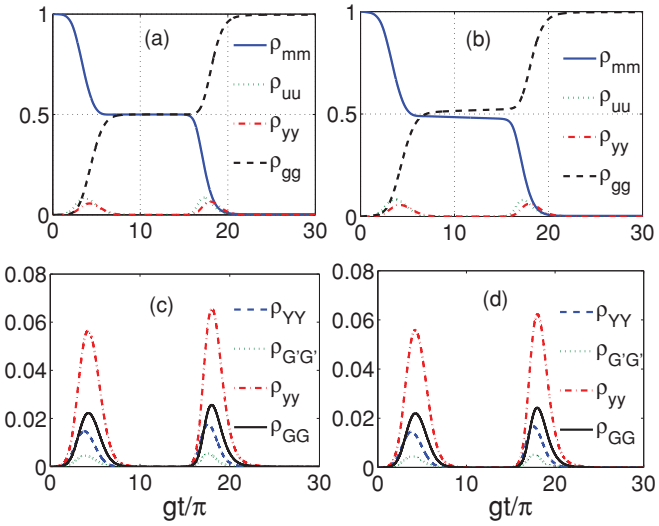

FIG. 2. (Color online) In (a) and (b), we show the populations in state $|m\rangle$ (blue solid line), in state $|g\rangle$ (black dashed line), in state $|y\rangle$ (red chain line), and in state $|u\rangle$ (green dotted line) during the evolution. In (c) and (d), the populations in states $|Y\rangle$, $|G\rangle$, and $|G'\rangle$ are compared with the population in state $|y\rangle$. We use the following parameters: $g_1 = g_2 = g$, $\kappa = 2.5g$, $\gamma_2 = \gamma_1 = 10^{-3}g$, $\gamma_d = 10^{-2}g$, $\Delta_1 = -3g$, $\Delta_2 = 2g$, $\Delta_p = -1.5g$, $\Omega_1(t)/g = 0.68\exp[-(t-2\tau_p)^2/\tau_p^2]$, $\Omega_2(t)/g = 3\exp[-(t-9.5\tau_p)^2/\tau_p^2]$, and $g\tau_p = 2\pi$; for (a) and (c), $\gamma_m = 0$, while for (b) and (d), $\gamma_m = 10^{-3}g$.

frequency of each pulse and T is the time gap between the pulses. We select a typical value of $\Omega_1(t)$ such that the population of the state $|m\rangle$ is pumped to the state $|y,1\rangle$ in CAPAP with probability $p_1 \approx 1/2$. Due to the nature of the leaky cavity mode, the photon is emitted from the final state $|y,1\rangle$ and the system is evolved into the state $|y,0\rangle$ state. The population in state $|y,0\rangle$ is then transferred to the state $|g,1\rangle$ through the cavity mode. After emitting another photon from the state $|g,1\rangle$, the system finally reaches the ground state $|g,0\rangle$. In order to avoid the reabsorption of the emitted photons by the cavity mode, and excitation of the transition $|y,1\rangle \rightarrow |g,2\rangle$, the decay rate of the cavity mode should be larger than the cavity-exciton coupling rate ($\kappa \gg g$), i.e., the cavity is in the weak coupling limit. Thus a photon pair in the early time bin is emitted during the interaction of the first pulse $\Omega_1(t)$. The remaining population in state $|m\rangle$ is similarly pumped by the subsequent pulse $\Omega_2(t-T)$ and a photon pair is generated with probability $p_2 \approx 1 - p_1$ in the *late* time bin. The state of the generated photon pair is now a maximally time-bin entangled state. In Figs. 2(a) and 2(c), we consider the metastable state $|m\rangle$ as a dark exciton ($\gamma_m = 0$) and, in Figs. 2(b) and 2(d), we consider state $|m\rangle$ as an off-resonant exciton with small radiative decay (e.g., in a photonic crystal slab system). In the presence of a small decay of the metastable state, the probability of generating a photon pair in the second pulse p_2 is only slightly reduced. For a QD embedded in a photonic crystal microcavity, the spontaneous decay rate of the off-resonant exciton has values of 0.05–0.1 μeV (smaller than $10^{-3}g$ for $g = 0.1$ meV), and the cavity decay condition $\kappa \gg g$ is achieved. All of these parameters correspond closely to those in present day experiments.[24]

During the interaction time with the pump pulses, the population in the upper state $|u\rangle$ remains always less than 0.1 and the population in $|g,2\rangle$ remains negligible. The state of the emitted photon pair from the cavity mode can therefore be written as

$$|\psi(t)\rangle = [a_1^\dagger(t)a_2^\dagger(t) + a_1^\dagger(t-T)a_2^\dagger(t-T)]|\{0\}\rangle, \quad (4)$$

where $|\{0\}\rangle$ is the vacuum field, $\langle a_1(t)\rangle = \langle\sigma_{yY}(t)\rangle$, and $\langle a_2(t)\rangle = \langle\sigma_{gG}(t)\rangle$, with $\sigma_{ij} = |i\rangle\langle j|$. In quantum-information protocols, such as entanglement swapping, it is essential that the photons in the modes a_1 and a_2 should not have any other correlation except the time-bin entanglement. However, in the biexciton-exciton cascade, the a_2 mode photon is always generated after the emission of the a_1 mode photon. Thus the a_1 and a_2 modes remain time correlated. This undesirable temporal correlation becomes negligible for $\Gamma_1/\Gamma_2 \gg 1$,[15] where Γ_i is the emission rate of the photon in a_i mode. In our scheme above, the first photon in mode a_1 is generated in the resonant two-photon process, which is emitted with the cavity-mode decay rate κ, and the second photon is generated through cavity-enhanced spontaneous emission. The condition $\Gamma_1/\Gamma_2 \gg 1$ can therefore be satisfied by choosing $g_2^2/(\kappa^2 + \Delta_2^2) \ll 1$.

III. TRIPLE COINCIDENT DETECTION OF THE PHOTON ENTANGLEMENT AND THE INFLUENCE OF PURE DEPHASING

Next, we discuss how to measure and calculate the entanglement of the generated state of the photons. The concurrence of the state (4) is directly related to the coherence of the state.[12] For measuring the degree of entanglement, photons from each mode are passed through an unbalanced two-path interferometer;[5] the time difference between the two arms is T, with phase difference ϕ, and T is similar to the time difference between the two pulses in the pump fields. After passing through the interferometer, the field operators at the output of the interferometer can be expressed as

$$a_3(t) = a_1(t) + e^{i\phi}a_1(t-T), \quad (5)$$

$$a_4(t) = a_2(t) + e^{i\phi}a_2(t-T). \quad (6)$$

The postselection, for detecting both photons simultaneously after passing through the interferometers, projects the state (4) into the following state:

$$|\psi_c(t)\rangle = [a_1^\dagger(t)a_2^\dagger(t) + (1+e^{2i\phi})a_1^\dagger(t-T)a_2^\dagger(t-T) + a_1^\dagger(t-2T)a_2^\dagger(t-2T)]|\{0\}\rangle. \quad (7)$$

Clearly, the state (7) has three terms that are distinguishable in time. The middle term, appearing at $t = T$, provides the information about the entanglement of state (4). For separating different terms in state (7), the time of detection of the photons is measured with reference to the pump photons using a triple coincidence detection. The probability of triple coincidence detection of one photon at each output of the interferometer, and one from the input pulse Ω_1, is given by

$$G^{(3)}(\tau) = \int_0^\infty dt' \int_{-T_{\rm bin}}^{T_{\rm bin}} d\tau' |\Omega_1(t')|^2 \langle a_3^\dagger(t'+\tau)a_4^\dagger(t'+\tau+\tau')a_4(t'+\tau+\tau')a_3(t'+\tau)\rangle, \quad (8)$$

where $T_{\rm bin}$ is the width of the time bins, which is chosen larger than the biexciton-exciton cascade decay and smaller than T. We can simplify the above expression for $G^{(3)}(\tau)$ using the property of field operators, $a_1(t)a_2(t-T)|\{0\}\rangle = 0$, as both photons are generated almost together in the cascade decay. Subsequently, we can simplify the correlation function in Eq. (8) as

$$\begin{aligned}\langle a_3^\dagger(t'+\tau)a_4^\dagger(t'+\tau+\tau')a_4(t'+\tau+\tau')a_3(t'+\tau)\rangle &= \langle a_1^\dagger(t'+\tau)a_2^\dagger(t'+\tau+\tau')a_2(t'+\tau+\tau')a_1(t'+\tau)\rangle \\ &+ \langle a_1^\dagger(t'-T+\tau)a_2^\dagger(t'-T+\tau+\tau')a_2(t'-T+\tau+\tau')a_1(t'-T+\tau)\rangle + 2\cos 2\phi\langle a_1^\dagger(t'+\tau)a_2^\dagger(t'+\tau+\tau')a_2(t'-T+\tau+\tau')a_1(t'-T+\tau)\rangle, \end{aligned} \quad (9)$$

which is evaluated for state (4) by applying the quantum regression theorem.[32] We relegate the details of the $G^{(3)}$ calculation to the Appendix.

In Fig. 3(a), we plot $G^{(3)}(\tau)$ for the same parameters used in Fig. 2, where the time-dependent populations were shown. The computed value of $G^{(3)}(\tau)$ has three peaks centered at $\tau = 0$, T, and $2T$. The first peak at $\tau = 0$ corresponds to the photons generated in the early time bin that have passed through the short arms of the interferometers. Similarly, the peak centered at $\tau = 2T$ corresponds to the photon pairs generated in the late time bin that have passed through the long arms of the interferometers. The central peak at $\tau = T$ corresponds to the overlap of the photons generated in the early time bin and passed through the longer arms in the interferometers and the photons generated in the late time bin and passed through the short arms. Thus only the central peak contains the information about the entanglement and can be easily selected by choosing a narrow time window around $\tau = T$. We have

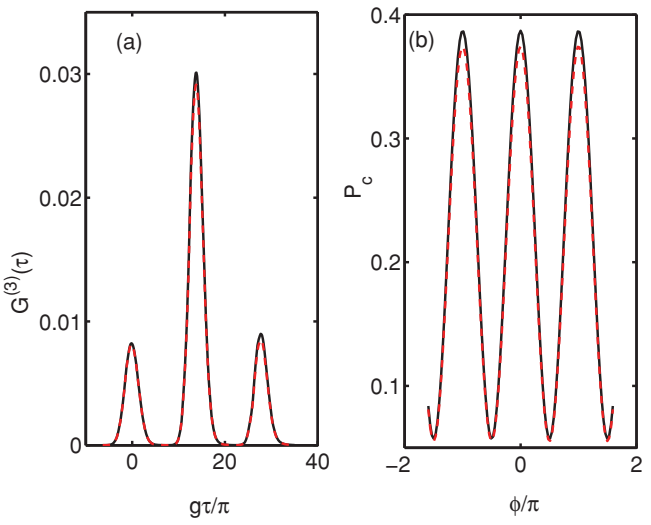

FIG. 3. (Color online) In (a), the triple coincidence correlation of detecting one photon at each output port of the interferometer and one from the input pulse Ω_1 for $T = 14\pi/g$. In (b), the integrated values of the triple coincidence correlation $G^{(3)}(\tau)$ along the central peak at $\tau = T$ are shown. The interference pattern appears on changing the phase ϕ produced by the interferometers. The solid black curve is for $\gamma_m = 0$ and the red dashed curve is for $\gamma_m = 10^{-3}g$. The other parameters are the same as in Fig. 2.

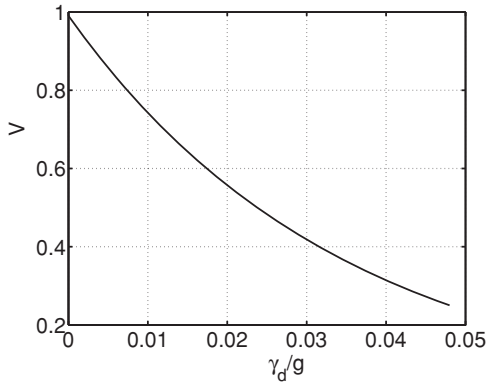

FIG. 4. Dependence of the visibility, i.e., entanglement, of the generated time-bin entangled state of the photon on dephasing rate γ_d.

also found that the required value of T is slightly less than the actual time between the pump pulses, which shows that in CAPAP, the photons are actually generated before the pump pulse reaches its maximum. For the parameters used in Fig. 2, the time between pump pulses is $15\pi/g$, but the central peak in Fig. 3(a) is a maximum for $T = 14\pi/g$.

The coherence in the generated state (4) can be measured by varying the phase ϕ between the overlapping amplitudes corresponding to the early and the late time bins along the central peak. In Fig. 3(b), we plot the interference pattern produced in the measurement of $P_c = \int_{T-T_{\rm bin}}^{T+T_{\rm bin}} G^{(3)}(\tau)d\tau$. The visibility of the interference pattern, defined as $V =$ (maximum of P_c − minimum of P_c)/(maximum of P_c + minimum of P_c), gives the concurrence and the purity of the generated state (4). For smaller values of γ_m, we find negligible changes (red dashed line) in the values of $G^{(3)}(\tau)$. The spontaneous decay of the metastable state cannot induce dephasing in the generated entangled state as the coherence in the state is transcribed by the input pulses.

In Fig. 4, we show the dependence of the visibility on the dephasing rate. In the presence of pure dephasing, the visibility—i.e., concurrence of the generated state [Eq. (4)]—is strongly inhibited. Further, the dephasing in the state [Eq. (4)] only occurs during the interaction of the pump pulses. The dephasing during the time gap between the pump pulses plays no role as the coherence in the state is produced by the coherence between the input pulses. The inhibition of interference due to dephasing can be understood as due to pure dephasing (e.g., phonon bath interactions), which influences the information about the photons generated in different time bins. However, for the small dephasing rate $\gamma_d \approx 0.01 g_1$, the value of the visibility is larger than $1/\sqrt{2}$, which is the required threshold for violation of Bell's inequalities.[33] In the presence of small spontaneous decay of the metastable state $|m\rangle$, the visibility remains unaffected.

IV. CONCLUSIONS

We have presented a cavity-QED scheme for generating a scalable source of time-bin entangled photon pairs, and we also investigated the role of pure dephasing on the entanglement. The generated state of the photons can be detected by measuring the correlations between the pump and the generated photons. We found that, for relatively small values of pure dephasing, it is possible to achieve large values of time-bin entanglement using present-day QD-cavity systems. An additional advantage of this biexciton-cascade cavity system is that coherently triggered single photons can be also produced using a single excitation pulse.[34]

ACKNOWLEDGMENTS

This work was supported by the National Sciences and Engineering Research Council of Canada and the Canadian Foundation for Innovation. We acknowledge useful discussions with Robin Williams and Gregor Weihs.

APPENDIX: CALCULATION OF MULTITIME CORRELATIONS

Here we briefly discuss the method for calculating the two-time correlation and four-time correlation used in Sec. III. We follow the approach discussed by Gardiner and Zoller[32] for evaluating multitime correlations. The required two-time correlation can be expressed as

$$\begin{aligned}&\langle a_1^\dagger(t)a_2^\dagger(t+\tau)a_2(t+\tau)a_1(t)\rangle\\&\quad= \mathrm{Tr}\{a_2(t+\tau)a_1(t)\rho(0)a_1^\dagger(t)a_2^\dagger(t+\tau)\}\\&\quad= \mathrm{Tr}\{a_2(t+\tau)\rho'(t)a_2^\dagger(t+\tau)\}\\&\quad= \mathrm{Tr}\{a_2\rho'(t+\tau)a_2^\dagger\},\end{aligned}\tag{A1}$$

where Tr stands for trace and operators a_i appearing without time parentheses are in the Schrödinger picture; $\rho'(t) = a_1(t)\rho(0)a_1^\dagger(t) = a_1\rho(t)a_1^\dagger$ is calculated after evolving the initial state $\rho(0) = \rho_{mm}|m\rangle\langle m|$ for time t using Eqs. (3a)–(3n) and then operating by a_1 and $a_1^\dagger$ from left and right, respectively. Additionally, ρ' also follows the same equations of motion (3a)–(3n). Using the initial value $\rho'(t) = a_1\rho(t)a_1^\dagger$ at time t, and evolving for time τ, $\rho'(t+\tau)$ is calculated. The value of the required correlation is calculated using Eq. (A1). A similar approach, considering the times appearing in the a operators in ascending order, is applied in evaluating the four-time correlations:

$$\begin{aligned}&\langle a_1^\dagger(t)a_2^\dagger(t+\tau)a_2(t-T+\tau)a_1(t-T)\rangle\\&\quad= \mathrm{Tr}\{a_2(t-T+\tau)a_1(t-T)\rho(0)a_1^\dagger(t)a_2^\dagger(t+\tau)\}\\&\quad= \mathrm{Tr}\{a_2(t-T+\tau)\rho_1(t-T)a_1^\dagger(t)a_2^\dagger(t+\tau)\}\\&\quad= \mathrm{Tr}\{\rho_2(t-T+\tau)a_1^\dagger(t)a_2^\dagger(t+\tau)\}\\&\quad= \mathrm{Tr}\{\rho_3(t)a_2^\dagger(t+\tau)\}\\&\quad= \mathrm{Tr}\{\rho_3(t+\tau)a_2^\dagger\},\end{aligned}\tag{A2}$$

where $\rho(0) = \rho_{mm}|m\rangle\langle m|$, $\rho_1(t-T) \equiv a_1(t-T)\rho(0) \equiv a_1\rho(t-T)$, $\rho_2(t-T+\tau) \equiv a_2(t-T+\tau)\rho_1(t-T) \equiv a_2\rho_1(t-T+\tau)$, and $\rho_3(t) \equiv \rho_2(t-T+\tau)a_1^\dagger(t) \equiv \rho_2(t)a_1^\dagger$. Thus the density matrices ρ, ρ_1, ρ_2, and ρ_3 are evolved for times 0 to $t-T$, $t-T$ to $t-T+\tau$, $t-T+\tau$ to t, and t to $t+\tau$, respectively. The evolution of $\rho(0)$ is given by Eqs. (3a)–(3n), while the evolutions of density matrices ρ_i for $i = 1,2$, and 3 follow the similar equations, written

for ρ, as

$$\dot{\rho}_{Yy} = -ig_1\rho_{uy} - ig_2\sqrt{2}\rho_{G'y} + ig_2\rho_{YG} - (\gamma_2 + \kappa/2 + \gamma_d)\rho_{Yy}, \quad \text{(A3)}$$

$$\dot{\rho}_{G'G} = -ig_2\sqrt{2}\rho_{YG} + ig_2\rho_{G'y} - \tfrac{3}{2}\kappa\rho_{G'G}, \quad \text{(A4)}$$

$$\dot{\rho}_{Gg} = -ig_2\rho_{yg} - \tfrac{1}{2}\kappa\rho_{Gg}, \quad \text{(A5)}$$

$$\dot{\rho}_{uy} = -i\Delta_1\rho_{uy} - i\Omega_p(t)\rho_{my} - ig_1\rho_{Yy} + ig_2\rho_{uG} - (\gamma_1 + \gamma_2/2 + 3\gamma_d/2)\rho_{uy}, \quad \text{(A6)}$$

$$\dot{\rho}_{G'y} = i\Delta_2\rho_{G'y} - ig_2\sqrt{2}\rho_{Yy} + ig_2\rho_{G'G} - (\kappa + \gamma_2/2 + \gamma_d/2)\rho_{G'y}, \quad \text{(A7)}$$

$$\dot{\rho}_{YG} = -i\Delta_2\rho_{YG} - ig_1\rho_{uG} - ig_2\sqrt{2}\rho_{G'G} + ig_2\rho_{Yy} - (\kappa + \gamma_2/2 + \gamma_d/2)\rho_{YG}, \quad \text{(A8)}$$

$$\dot{\rho}_{yg} = -i\Delta_2\rho_{yg} - ig_2\rho_{Gg} - \tfrac{1}{2}(\gamma_2 + \gamma_d)\rho_{yg}, \quad \text{(A9)}$$

$$\dot{\rho}_{my} = -i(\Delta_1 - \Delta_p)\rho_{my} - i\Omega_p^*(t)\rho_{uy} + ig_2\rho_{mG} - (\gamma_m/2 + \gamma_2/2 + \gamma_d)\rho_{my}, \quad \text{(A10)}$$

$$\dot{\rho}_{uG} = -i(\Delta_1 + \Delta_2)\rho_{uG} - i\Omega_p\rho_{mG} - ig_1\rho_{YG} + ig_2\rho_{uy} - (\kappa/2 + \gamma_1 + \gamma_d)\rho_{uG}, \quad \text{(A11)}$$

$$\dot{\rho}_{mG} = -i(\Delta_1 + \Delta_2 - \Delta_p)\rho_{mG} - i\Omega_p^*(t)\rho_{uG} + ig_2\rho_{my} - \tfrac{1}{2}(\kappa + \gamma_m + \gamma_d)\rho_{mG}, \quad \text{(A12)}$$

$$\dot{\rho}_{G'g} = -ig_2\sqrt{2}\rho_{Yg} - \kappa\rho_{G'g}, \quad \text{(A13)}$$

$$\dot{\rho}_{Yg} = -i\Delta_2\rho_{Yg} - ig_2\sqrt{2}\rho_{G'g} - ig_1\rho_{ug} - \tfrac{1}{2}(\kappa + \gamma_2 + \gamma_d)\rho_{Yg}, \quad \text{(A14)}$$

$$\dot{\rho}_{ug} = -i(\Delta_1 + \Delta_2)\rho_{ug} - i\Omega_p\rho_{mg} - ig_1\rho_{Yg} - (\gamma_1 + \gamma_d)\rho_{ug}, \quad \text{(A15)}$$

$$\dot{\rho}_{mg} = -i(\Delta_1 + \Delta_2 - \Delta_p)\rho_{mg} - i\Omega_p^*(t)\rho_{ug} - \tfrac{1}{2}(\gamma_m + \gamma_d)\rho_{mg}. \quad \text{(A16)}$$

Finally, the value of four-time correlations used in Sec. III are found using Eq. (A2).

[1] W. Tittel and G. Weihs, Quant. Inf. Comp. **1-2**, 3 (2001); M. A. Nielsen, and I. L. Chuang, *Quantum Computation and Quantum Information* (Cambridge University Press, Cambridge, UK, 2000).

[2] A. K. Ekert, Phys. Rev. Lett. **67**, 661 (1991); T. Jennewein, C. Simon, G. Weihs, H. Weinfurter, and A. Zeilinger, *ibid.* **84**, 4729 (2000); D. S. Naik, C. G. Peterson, A. G. White, A. J. Berglund, and P. G. Kwiat, *ibid.* **84**, 4733 (2000).

[3] C. H. Bennett, G. Brassard, C. Crépeau, R. Jozsa, A. Peres, and W. K. Wootters, Phys. Rev. Lett. **70**, 1895 (1993); D. Bouwmeester, J.-W. Pan, K. Mattle, M. Eibl, H. Weinfurter, and A. Zeilinger, Nature (London) **390**, 575 (1997); D. Boschi, S. Branca, F. De Martini, L. Hardy, and S. Popescu, Phys. Rev. Lett. **80**, 1121 (1998).

[4] P. G. Kwiat, K. Mattle, H. Weinfurter, A. Zeilinger, A. V. Sergienko, and Y. Shih, Phys. Rev. Lett. **75**, 4337 (1995).

[5] W. Tittel, J. Brendel, H. Zbinden, and N. Gisin, Phys. Rev. Lett. **81**, 3563 (1998).

[6] J. Brendel, N. Gisin, W. Tittel, and H. Zbinden, Phys. Rev. Lett. **82**, 2594 (1999); W. Tittel, J. Brendel, H. Zbinden, and N. Gisin, *ibid.* **84**, 4737 (2000).

[7] I. Marcikic, H. de Riedmatten, W. Tittel, V. Scarani, H. Zbinden, and N. Gisin, Phys. Rev. A **66**, 062308 (2002).

[8] I. Marcikic, H. de Riedmatten, W. Tittel, H. Zbinden, M. Legré, and N. Gisin, Phys. Rev. Lett. **93**, 180502 (2004).

[9] L. Mandel and E. Wolf, *Optical Coherence and Quantum Optics* (Cambridge University Press, Cambridge, England, 1995).

[10] P. Zoller, Th. Beth, D. Binosi, R. Blatt, H. J. Briegel, D. Bruss, T. Calarco, J. I. Cirac, D. Deutsch, J. Eisert, A. Ekert, C. Fabre, N. Gisin, P. Grangiere, M. Grassl, S. Haroche, A. Imamoglu, A. Karlson, J. Kempe, L. Kouwenhoven, S. Kröll, G. Leuchs, M. Lewenstein, D. Loss, N. Lütkenhaus, S. Massar, J. E. Mooij, M. B. Plenio, E. S. Polzik, S. Popescu, G. Rempe, A. Sergienko, D. Suter, J. Twamley, G. Wendin, R. Werner, A. Winter, J. Wrachtrup, and A. Zeilinger, Eur. Phys. J. D **36/2**, 203 (2005).

[11] C. Santori, D. Fattal, J. Vuckovic, G. S. Solomon, and Y. Yamamoto, Nature (London) **419**, 594 (2002); D. Fattal, K. Inoue, J. Vuckovic, C. Santori, G. S. Solomon, and Y. Yamamoto, Phys. Rev. Lett. **92**, 037903 (2004); R. B. Patel, A. J. Bennett, K. Cooper, P. Atkinson, C. A. Nicoll, D. A. Ritchie, and A. J. Shields, *ibid.* **100**, 207405 (2008).

[12] N. Akopian, N. H. Lindner, E. Poem, Y. Berlatzky, J. Avron, D. Gershoni, B. D. Gerardot, and P. M. Petroff, Phys. Rev. Lett. **96**, 130501 (2006).

[13] R. M. Stevenson, R. J. Young, P. Atkinson, K. Cooper, D. A. Ritchie, and A. J. Shields, Nature (London) **439**, 179 (2006); A. J. Hudson, R. M. Stevenson, A. J. Bennett, R. J. Young, C. A. Nicoll, P. Atkinson, K. Cooper, D. A. Ritchie, and A. J. Shields, Phys. Rev. Lett. **99**, 266802 (2007).

[14] A. Dousse, J. Suffczynski, O. Krebs, A. Beveratos, A. Lemaitre, I. Sagnes, J. Bloch, P. Voisin, and P. Senellart, Appl. Phys. Lett. **97**, 081104 (2010); A. Muller, W. Fang, J. Lawall, and G. S. Solomon, Phys. Rev. Lett. **103**, 217402 (2009); R. Hafenbrak, S. M. Ulrich, P. Michler, L. Wang, A. Rastelli, and O. G. Schmidt, New J. Phys. **9**, 315 (2007).

[15] C. Simon and J. P. Poizat, Phys. Rev. Lett. **94**, 030502 (2005).

[16] A. Kuhn, M. Hennrich, and G. Rempe, Phys. Rev. Lett. **89**, 067901 (2002); J. McKeever, A. Boca, A. D. Boozer, R. Miller, J. R. Buck, A. Kuzmich, and H. J. Kimble, Science **303**, 1992 (2004); M. Hijlkema *et al.*, Nat. Phys. **3**, 253 (2007).

[17] S. Zhdanovich, E. A. Shapiro, J. W. Hepburn, M. Shapiro, and V. Milner, Phys. Rev. A **80**, 063405 (2009); S. Zhdanovich, E. A. Shapiro, M. Shapiro, J. W. Hepburn, and V. Milner, Phys. Rev. Lett. **100**, 103004 (2008); E. A. Shapiro, V. Milner, C. Menzel-Jones, and M. Shapiro, *ibid.* **99**, 033002 (2007).

[18] E. B. Flagg, A. Muller, J. W. Robertson, S. Founta, D. G. Deppe, M. Xiao, W. Ma, G. J. Salamo, and C. K. Shih, Nat. Phys. **5**, 203 (2009).

[19] S. Ates, S. M. Ulrich, S. Reitzenstein, A. Löffler, A. Forchel, and P. Michler, Phys. Rev. Lett. **103**, 167402 (2009); S. Ates, S. M.

Ulrich, A. Ulhaq, S. Reitzenstein, A. Löffler, S. Höfling, A. Forchel, and P. Michler, Nat. Photon. **3**, 724 (2009).

[20]A. Muller, E. B. Flagg, P. Bianucci, X. Y. Wang, D. G. Deppe, W. Ma, J. Zhang, G. J. Salamo, M. Xiao, and C. K. Shih, Phys. Rev. Lett. **99**, 187402 (2007).

[21]K. Srinivasan, C. P. Michael, R. Perahia, and O. Painter, Phys. Rev. A **78**, 033839 (2008).

[22]D. Englund, A. Majumdar, A. Faraon, M. Toishi, N. Stoltz, P. Petroff, and J. Vuckovic, Phys. Rev. Lett. **104**, 073904 (2010).

[23]E. Poem, Y. Kodriano, C. Tradonsky, N. H. Lindner, B. D. Gerardot, P. M. Petroff, and D. Gershoni, Nat. Phys. **6**, 993 (2010); M. Reischle, G. J. Beirne, R. Roßbach, M. Jetter, and P. Michler, Phys. Rev. Lett. **101**, 146402 (2008); J. Johansen, B. Julsgaard, S. Stobbe, J. M. Hvam, and P. Lodahl, Phys. Rev. B **81**, 081304(R) (2010).

[24]K. Hennessy, A. Badolato, M. Winger, D. Gerace, M. Atatüre, S. Gulde, S. Fält, E. L. Hu, and A. Imamoğlu, Nature (London) **445**, 896 (2007).

[25]P. K. Pathak and S. Hughes, Phys. Rev. B **80**, 155325 (2009).

[26]M. E. Reimer, M. Korkusinski, D. Dalacu, J. Lefebvre, J. Lapointe, P. J. Poole, G. C. Aers, W. R. McKinnon, P. Hawrylak, and R. L. Williams, Phys. Rev. B **78**, 195301 (2008).

[27]S. Rodt, R. Heitz, A. Schliwa, R. L. Sellin, F. Guffarth, and D. Bimberg, Phys. Rev. B **68**, 035331 (2003).

[28]F. Ding, R. Singh, J. D. Plumhof, T. Zander, V. Krapek, Y. H. Chen, M. Benyoucef, V. Zwiller, K. Dorr, G. Bester, A. Rastelli, and O. G. Schmidt, Phys. Rev. Lett. **104**, 067405 (2010).

[29]V. Stavarache, D. Reuter, A. D. Wieck, M. Schwab, D. R. Yakovlev, R. Oulton, and M. Bayer, Appl. Phys. Lett. **89**, 123105 (2006); X. Xu, A. Andreev, and D. A. Williams, New J. Phys. **10**, 053036 (2008); W. Heller, U. Bockelmann, and G. Abstreiter, Phys. Rev. B **57**, 6270 (1998).

[30]A. Faraon, A. Majumdar, H. Kim, P. Petroff, and J. Vuckovic, Phys. Rev. Lett. **104**, 047402 (2010).

[31]L. P. Yatsenko, S. Guérin, T. Halfmann, K. Böhmer, B. W. Shore, and K. Bergmann, Phys. Rev. A **58**, 4683 (1998); S. Guérin, L. P. Yatsenko, T. Halfmann, B. W. Shore, and K. Bergmann, *ibid*. **58**, 4691 (1998).

[32]C. W. Gardiner and P. Zoller, *Quantum Noise, A Handbook of Markovian and Non-Markovian Quantum Stochastic Methods with Applications to Quantum Optics* (Springer, Berlin, 2004).

[33]F. Verstraete and M. M. Wolf, Phys. Rev. Lett. **89**, 170401 (2002).

[34]P. K. Pathak and S. Hughes, Phys. Rev. B **82**, 045308 (2010).